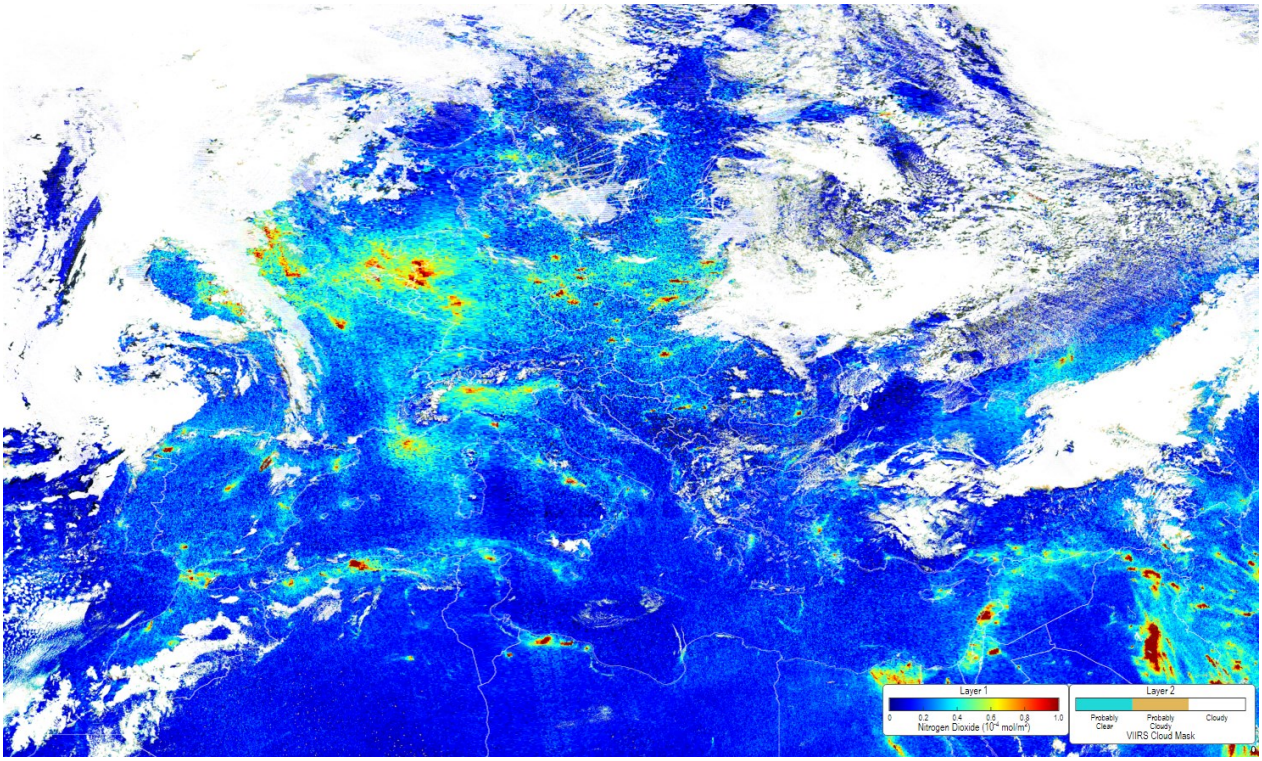

Composite image of S5P/TROPOMI tropospheric NO_2 columns over Europe [layer 1] and NOAA-20 cloud mask [layer 2] for the 19th of July 2022. From **https://www.star.nesdis.noaa.gov/jpss/mapper/index.php**.

3DCTRL project

Requirements Baseline Document (D1)

Doc. ID	3DCTRL_RBD_D1
Issue	1.0
Date	22.09.2022
Prepared by	M. Koukouli (AUTH), A. Doicu (DLR), D. Efremenko (DLR), C. Emde (LMU), H. Yuan (BIRA), D. Karagkiozidis (AUTH) and A. Kylling (NILU)
Status	Final

Aristotle University of Thessaloniki – Laboratory of Astrophysics | AUTH-LAP
German Aerospace Centre - Remote Sensing Technology Institute | DLR-IMF
Ludwig-Maximilians-University in Munich | LMU
Norwegian Institute for Air Research | NILU
Royal Belgian Institute for Space Aeronomie | BIRA-IASB

3DCTRL | ESA contract number 4000137834/22/I-AG

DOCUMENT APPROVAL RECORD

	Digital signature:
Prepared by: MariLiza Koukouli	Maria-Elissavet Koukouli Digitally signed by Maria-Elissavet Koukouli Date: 2022.09.22 12:20:05 +03'00'
Checked by:	

DOCUMENT CHANGE RECORD

Issue	Date	Change
0.9	04.08.2022	First initial version
1.0	14.09.2022	Final version

TABLE OF CONTENTS

LIST OF FIGURES

LIST OF TABLES

1. Introduction

1.1 Purpose

This document is the Requirements Baseline Document (Deliverable D1) as part of the 3DCTRL project. This document consolidates the preliminary scientific requirements for the 3DCTRL project, including a detailed review, assessment and cross-comparison of existing relevant products, a survey of all accessible associated datasets, current and ongoing initiatives and projects related to the treatment of clouds in trace gas retrieval algorithms, as well as a consolidated risk analysis pointing out which risk areas could affect the final success of the project. This document represents the basis for all the activities to be carried out during the project.

1.2 References

1.2.1 Applicable Documents

The following project documents contain provisions which, through reference in this text, become applicable to the extent specified in this document.

Table 1 Applicable Documents

Document Title		Document ID	Issue
[AD01]	ESA Invitation to Tender for Atmosphere Science Cluster – Research Opportunities 2 – Expro+	ESA-CIP-POE-AG-535-cb-LE	1.0 (28/07/2021)

1.2.2 Reference Documents

The documents are referenced in this document. They have been used (in the sense of tailoring) to prepare the document on hand.

Table 2 Reference Documents

Title		Document ID	Issue
[RD01]	TROPOMI ATBD of the total and tropospheric NO2 data products	S5P-KNMI-L2-0005-RP	2.4.0
[RD02]	Sentinel-5 precursor/TROPOMI Level 2 Product User Manual Nitrogendioxide	S5P-KNMI-L2-0021-MA	4.1.0
[RD03]	S5P Mission Performance Centre Nitrogen Dioxide [L2 NO2] Readme	S5P-MPC-KNMI-PRF-NO2	2.2
[RD04]	Sentinel-5P TROPOMI CLOUD ATBD	S5P-DLR-L2-ATBD-400I	2.3

1.3 Terms and Abbreviations

Abbreviations specific to the report are found in the following table:

Abbreviation	Meaning
(V) LIDORT	(Vector) Linearized Discrete Ordinate Radiative Transfer
AK	Averaging kernel
AMF	Airmass factor
ATBD	Algorithm Theoretic Baseline Document
BIRA-IASB	Royal Belgian Institute for Space Aeronomy
CTM	Chemical transport model
DLR	German Aerospace Centre
DOAS	Differential Optical Absorption Spectroscopy
dSCD	Differential slant column density
FM	Forward model
KNMI	Royal Netherlands Meteorological Institute
libRadtran	library for radiative transfer
LAP/AUTH	Laboratory of Atmospheric Physics, Aristotle University of Thessaloniki
LIDAR	Light Detection And Ranging
LUT	Look-up table
MAX-DOAS	Multi Axis Differential Optical Absorption Spectroscopy
MYSTIC	Monte Carlo code for the phYSically correct Tracing of photons In Cloudy atmospheres
NIR	Near-infrared
NISA	Nonlocal Independent Slice Approximation
NRT	Near-real time
OCRA	Optical Cloud Recognition Algorithm
paNTICA	nonlocal tilted independent column approximation
ROCINN	Retrieval of Cloud Information using Neural Networks
RTE	Radiative Transfer Equation
RTM	Radiative Transfer Model
RTTOV	Radiative Transfer for TOVS
S5 L2PP	Sentinel-5 Level 2 Prototype Processors
S5P	Sentinel-5 Precursor
SCD	Slant column density
SHDOM	Spherical harmonics discrete ordinate method
TICA	Tilted Independent Column Approximation
TROPOMI	Tropospheric Ozone Measurement Instrument

Abbreviation	Meaning
UV	Ultraviolet
VCD	Vertical column density
VIS	Visible

2. The 3DCTRL project

The *Handling of 3D Clouds in Trace Gas Retrievals*, 3DCTRL project is dedicated to improving the handling of clouds in trace gas retrievals, specifically the retrieval of tropospheric NO_2 columns. This trace gas is of great interest to the scientific, but also the air quality forecast modelling community, as it is the major air quality marker. The current operational S5P/TROPOMI tropospheric NO_2 product developers suggest that a filter be applied to the dataset[1] which basically rejects all cloud-covered scenes, with a cloud radiance fraction > 0.5, i.e. a cloud fraction > 0.2. As a result, during the winter months especially, entire days of crucial space-borne observations are excluded from further analysis and consideration. For this reason, the 3DCTRL project is aiming to demonstrate that realistic cloud treatments can be introduced into the operational retrieval analysis chains both for current, such as S5P/TROPOMI, as well as future, such as Sentine-4 and -5, missions.

The major goals of the 3DCTRL project are:

i. to evaluate cloud correction methodologies in Copernicus Sentinel-4, Sentinel-5 and Sentinel-5p trace gas retrieval schemes, and
ii. to explore ways to improve handling of realistic clouds in the retrievals of atmospheric species.

The first goal of 3DCTRL is to evaluate the performance of currently used operational retrieval algorithms for Sentinel-4, Sentinel-5, and Sentinel-5p. In the recent ESA-funded study *Impact of 3D Cloud Structures on the Atmospheric Trace Gas Products from UV-VIS Sounders* (3DCATS), synthetic and observational data were used to identify and quantify possible cloud-related bias in NO_2 tropospheric vertical column densities (TVCD). Cloud shadow fraction, cloud top height, cloud optical depth, solar zenith and viewing angles, were identified as the metrics being the most important in identifying 3D cloud impacts on NO_2 TVCD retrievals. For a solar zenith angle less than about 40° the synthetic data show that the NO_2 TVCD bias is typically below 10%. For larger solar zenith angles both synthetic and observational data often show NO_2 TVCD bias on the order of tens of %. Specifically, for clearly identified cloud shadow bands in the observational data, the NO_2 TVCD appears low-biased when the cloud shadow fraction > 0.0 compared to when the cloud shadow fraction is zero. For solar zenith angles between 50-60°, about 16% of TROPOMI pixels with high quality value NO_2 TVCD retrievals, were found to be impacted by cloud effects larger than 20%. In the proposed 3DCTRL, the current operational cloud retrieval algorithms, FRESCO, O2-O2 and OCRA/ROCINN, will be applied on the same synthetic dataset, so that their performance can directly be compared.

The second goal of 3DCTRL is to explore ways to improve handling of realistic clouds in the retrievals of atmospheric species by designing new retrieval algorithms that take into account 3D cloud scattering. The reason for the aforementioned large bias is that the majority of operational retrieval algorithms are based on the so-called independent pixel approximation (IPA). The IPA for an atmosphere exhibiting partial cloudiness means to compute separately the radiances for completely cloudy and clear skies, and then to express the partially cloudy radiance as a weighted sum of the separate radiances; the weighting factor being provided by cloud fraction. The clouds within each pixel are assumed to be plane-parallel and homogeneous in both horizontal and vertical directions. The main advantage of the IPA is its computational efficiency, since it requires the solution of only two independent one-dimensional radiative transfer problems. The disadvantage is that for cloudy scenes of small horizontal extent, the errors due to the three-dimensional effects may be very significant and fast and more accurate models accounting for the cloud inhomogeneities are crucial and will be developed during this project.

To reach these goals, 3DCTRL has the following main objectives:

a) Generate synthetic reference datasets in which true cloud properties including their 3D structure and vertical distribution are known by means of 3D radiative transfer simulations, realistic synthetic data of cloud properties will be obtained from LES model
b) Explore ways to improve the handling of realistic clouds in trace gas retrievals, specifically for NO_2

[1] https://sentinel.esa.int/documents/247904/3541451/Sentinel-5P-Nitrogen-Dioxide-Level-2-Product-Readme-File

c) Testing and evaluation of improved approaches for cloud correction by application on synthetic and real TROPOMI-S5P data

Objective (a) will be addressed by generating a set of synthetic Sentinel-S5P observations which will be consolidated, in the manner similarly shown in Kylling et al. 2020 and Emde et al. 2022. The first set of synthetic data includes a 2D cloud, for which the following cloud parameters will be varied: cloud optical thickness, cloud bottom height, cloud geometrical thickness, and effective radius of cloud droplets/crystals. The second set of synthetic data includes cloud properties simulated by the LES model ICON for a region covering Germany and parts of surrounding countries with a spatial resolution of approximately 1x1km². In the ESA-3DCATS project it has been shown by comparison with VIIRS observations that the simulated cloud properties from ICON are realistic in a statistical sense (Emde et al. 2022).

Objective (b) will be addressed by designing new algorithms for trace gas retrievals from S5P measurements by taking into account the influence of clouds. Specifically, we intend to focus on NO_2 retrieval algorithms for 3D cloudy scenes, and in this regard, to extend the results established in Doicu et al. (2021) by (I) considering a simplified retrieval algorithm and (ii) analyzing the accuracy and efficiency of the retrieval algorithms through a more comprehensive numerical analysis.

Objective (c) will be addressed by evaluating the handling of clouds in the NO_2 retrievals based on both synthetic and real data. The standard NO_2 retrieval including cloud correction approaches will be applied to a series of synthetic spectra generated from addressing objective (a). The radiative transfer settings in the NO_2 and cloud retrievals will be made as consistent as possible with those used to generate the synthetic data sets, in order to ensure that the differences between retrieved column and truth are due to the clouds, which include the uncertainty due to the simplified cloud correction approach and the 3D cloud effects. The evaluation will be performed for real observations using S5P/TROPOMI and NPP-VIIRS data.

In the following document, we first present a review and assessment of existing algorithms and products, separately for the radiative transfer models (section 3.1.1), the retrieval algorithms (section 3.1.2) and the output products of this project (section 3.1.3.) We then continue with a comprehensive discussion of the different satellite-based (section 3.2.1) and ground-based (section 3.2.2) validation datasets used for fulfilling the objectives of 3DCTRL, in which section the added value to the community is also summarized. The validation strategy, as currently envisioned, is discussed separately for the evaluation of the new retrieval algorithm for 3D cloudy scenes in section 4.1 and for the validation of the updated tropospheric NO_2 S5P/TROPOMI product in section 4.2. The scientific and dataset requirements are briefly presented in section 5, while section 6 includes a plausible risk analysis for the aims of the project.

3. 3DCTRL algorithms and products

This section provides a review, assessment and cross-comparison of existing relevant products, datasets, methods, models and algorithms related to the 3DCTRL project aims. It also summarizes related ranges of validity, constraints, drawbacks and challenges. This section is subdivided into two main sub-sections, one covering the radiative transfer algorithms and retrieval techniques used in this project and the other covering the different validation datasets used to verify the improvements in the output product.

3.1 Algorithms

This section summarizes algorithms that allow the computations of the radiance field, as well as the basic retrieval methods used in the project.

3.1.1 Radiative transfer models

3.1.1.1 SHDOM

The most efficient and widely used multi-dimensional deterministic method in the atmospheric sciences is the Spherical Harmonics Discrete Ordinate Method (SHDOM) developed by Evans (1998). The radiative transfer equation (RTE) is solved in the three-dimensional geometry iteratively by using the spherical harmonic and the discrete ordinate representations of the radiance field. The method combines the spherical harmonic and the discrete ordinate representation of the radiance field. The streaming of the radiation is accurately modeled in the discrete ordinate space, while the computation of the scattering integral is efficiently performed in the spherical harmonic space. Moreover, storing the source function as a spherical harmonic series at each grid point requires less computer memory as compared with a purely discrete ordinate method. The so-called adaptive grid technique improves the solution accuracy by increasing the spatial resolution in regions where the source function is changing more rapidly. DLR version of SHDOM includes two algorithms based on the plane parallel homogeneous approximation; the first one uses the Picard iteration method, while the second one uses the discrete ordinate method with matrix exponential.

During the time we improved the accuracy and efficiency of SHDOM. In Doicu et al., 2013a we analyzed a specific class of short characteristic methods, namely those methods which use only quantities from one cell, and implemented first- and high-order difference schemes equipped with interpolation and flux conservation error calculations. In Doicu et al., 2013b we extended SHDOM to the vector case (VSHDOM) to compute the Stokes vector. In Doicu et al, 2018 we designed linearized versions of SHDOM (LSHDOM) based on forward and forward-adjoint approaches. Essentially, LSHDOM was specialized for derivative calculations and radiative transfer problems involving the delta-M approximation, the TMS correction, and the adaptive grid splitting, and practical formulas for computing the derivatives in the spherical harmonics space were derived.

Although the SHDOM algorithm provides an accurate solution for arbitrary inhomogeneous scenes, the computations are time-consuming. That imposes difficulties in using SHDOM for processing of big amount of data. For instance, in our tests for a three-dimensional geometry, the retrieval algorithm based on linearized SHDOM takes about 14 hours, while the relative errors are below 0.05%. Even this approach can be applied for offline processing of selected cloudy scenes, the systematic utilization of SHDOM seem to be not efficient.

3.1.1.2 Independent slice approximations

As three dimensional RTMs are time-consuming, we consider two-dimensional RTMs, which provide the radiance field in the xz-plane. In particular, in the independent slice approximation (ISA), we consider the RTE in the two-dimensional geometry, while the transport along the y-axis is neglected. The optical parameters are taken for the slice corresponding to a chosen y-value (typically, the slice goes through the center of the instrument field of view).

In the nonlocal independent slice approximation (NISA) the resulting radiance field is the result of the averaging procedure of two-dimensional radiances taken at different values of y. We consider a uniform distribution smoothing kernel. Note that a similar idea was implemented in the parameterized nonlocal tilted

independent column approximation (paNTICA) by Wissmeier et al. (2013) and independent pixel approximation modified source (IPAMS) by Gabriel & Evans (1996). However, in our approach, we use fill two-dimensional computations for diffuse radiance, which is expected to be more accurate.

Note that ISA requires the solution of only one two-dimensional RTE, while for NISA, the RTM has to be solved for several slices.

3.1.1.3 Independent Column Approximations

In the Tilted Independent Column Approximation (TICA), a direct radiation is calculated in a single, independent column that is slanted toward the sun and the diffuse radiation is calculated in the vertical column. Direct and diffuse radiations are calculated in the tilted, independent columns that are slanted according to the solar zenith and azimuth angles; Nonlocal Tilted Independent Column Approximation (NTICA) accounts for the diffuse radiation transport between the tilted columns by convolving the TICA reflectances with a kernel function.

3.1.1.4 Stochastic RTM

In the stochastic RTMs, cloud fields are regarded as stochastic scattering media due to their internal inhomogeneity and stochastic geometry. The mean radiative properties in these media are obtained by analytical averaging of the radiative transfer equation and new transport equations, relating the statistical parameters of the clouds to those of the radiance field, are derived. These methods deliver an approximate solution of the problem but are computationally efficient. Stochastic radiative transfer has been in the focus of our research at DLR. In Doicu et al, 2014a we derived an nth-order stochastic model for the solar radiation problem and arbitrary cloud statistics, as well as its particularization to broken cloud fields in general, and in particular to homogeneous three-, two- and one-dimensional broken clouds. The stochastic radiative transfer equations, which are equivalent to the Levermore-Pomraning equations, were solved by using the discrete ordinate method with matrix exponential. In Doicu et al, 2014b we designed approximate models in stochastic radiative transfer theory. The independent column approximation and its modified version with a solar source computed in a full three-dimensional atmosphere were formulated in a stochastic framework and for arbitrary cloud statistics. In Efremenko et al, 2016; 2018 an algorithm for accurate retrieving ozone and clouds parameters has been designed based on the DLR stochastic radiative transfer models for broken clouds. Unlike the stochastic model of Titov (Titov, 1990) using the Monte-Carlo method, our model is equipped with a deterministic solver. Moreover, in the Levermore-Pomraning model (Pomraning, 1991), the equations are formulated for the radiances in clear sky and cloud whereas in our model the equations are constructed for the mean radiance values and its statistical moments, which are more meaningful for retrieval.

In the project we consider the stochastic RTM with the zeroth-order closure approximation, which assumes that the fluctuating parts of the radiance and the extinction coefficient are not correlated. The stochastic RTM leads to a two-dimensional RTE, and therefore computationally fast, as compared to the full three-dimensional RTM, e.g. SHDOM.

3.1.1.5 Monte Carlo Radiative Transfer code to generate synthetic TROPOMI

The 3D radiative transfer simulations will be carried out by the MYSTIC model (Mayer 2009, Emde et al. 2011) which is implemented as a radiative transfer solver in the libRadtran package (Mayer and Kylling 2005, Emde et al. 2016). It allows efficient simulations in high spectral resolution for domains including 3D cloud structures. In the 3DCATS project (Kylling et al 2020), MYSTIC was used to generate the synthetic dataset consisting of more than 200 combinations of parameters (sun-observer geometries representative for LEO and GEO orbits and surface albedos) (Emde et al 2022).

3.1.1.6 Vector LInerized Discrete Ordinate Radiative Transfer (VLIDORT) to calculate NO_2 AMF

VLIDORT (Vector-LInearized Discrete Ordinate Radiative Transfer) was developed by Rob Spurr at RT SOLUTIONS, Inc. The model is based on the discrete ordinate approach to solve the radiative transfer equation

in a multi-layered atmosphere, reducing the RTE to a set of coupled linear first order differential equations. Then, perturbation theory is applied to the discrete ordinate solution (Spurr et al., 2001). Intensity and partial derivatives of intensity with respect to atmospheric parameters and surface parameters (i.e. weighting functions) are determined for upwelling direction at TOA, for arbitrary angular direction. The pseudo-spherical formulation in VLIDORT corrects for the curved atmosphere in the solar and scattered beam (for single scattering, not for multiple scattering). In the project, VLIDORT is used to calculate AMF for the NO_2 retrieval.

3.1.2 Retrieval algorithms

3.1.2.1 Differential radiance model with internal smoothing

In the so called Differential Radiance Model with Internal smoothing (DRMI) (Doicu et al 2021), the measured and simulated differential spectra are fitted in the selected bands. The low degree polynomials are subtracted from the measured and simulated spectra. These polynomials account for the low-order spectral structure due to cloud and aerosol scattering, and also partially compensate for uncertainties in the surface albedo. The coefficients of the smoothing polynomials are computed as solutions of a least-square problem and are uniquely determined.

The residual between the simulated and measured spectra are associated with a linear combination of the correction spectra describing different kinds of instrumental effects and complex physical phenomena, such as polarization correction spectrum, under-sampling spectrum, offset correction spectrum and Ring spectrum. The amplitudes of the correction spectra are also found in the retrieval process.

Note that the retrieval is performed in the whole spectral band and so, this approach requires hyper-spectral computations across the selected absorption band, which can be time-consuming. To overcome this, the correlated-K and principal component analysis based acceleration techniques can be used. In particular, in Doicu et al., 2020a a spectral acceleration approach for the SHDOM is designed. This approach combines the correlated k-distribution method and some dimensionality reduction techniques applied on the optical parameters of an atmospheric system. Through a numerical analysis, it is shown that relative to the correlated k-distribution method, PCA in conjunction with a second-order of scattering approximation yields an acceleration factor of 12.

3.1.2.2 Differential Optical Absorption spectroscopy

In the DOAS approach (Platt & Stutz, 2008) the logarithm of the measured spectrum is represented as a sum of altitude-averaged absorption cross-sections, low-degree smoothing polynomial and correction spectra. The weights at the cross-sections are referred to as the slant columns. The slant column is connected with the vertical column via the air-mass factor. In the classical DOAS, the slant column and the air-mass factor are assumed to be wavelength independent, and that the air-mass factor is defined with respect to the a priori gaseous profile. The computations of the air-mass factor at a reference wavelength involve the estimation of the derivative of the radiance with respect to the gaseous number density. Thus, the advantage of this approach is that the time-consuming derivative computations have to be performed only at a single wavelength.

3.1.2.3 Summary of the Radiative Transfer Models

Table 3 summarizes the RTMs discussed extensively previously. For the 3DCTRL project, the scalar SHDOM model is used to compute synthetic measurements and reference solutions. The LSHDOM model can provide the estimation of the retrieval error when a full 3D RTM is used for the retrieval. Then, 2D RTMs (ISA, NISA, stochastic) as well as 1D models (TICA, NTICA) models are applied in the retrieval algorithm.

The retrieval algorithms considered in the study include DRMI and DOAS approaches. While DRMI approach is more accurate than DOAS, the latter is computationally faster. Later on, the majority of trace gas retrieval algorithms are based on the DOAS methodology.

Our preliminary analysis of the NO_2 retrieval results show that TICA requires 20 - 30 sec while the relative errors are of about 20%; the ISA algorithm takes 6-8 min providing relative errors below 5%. The TISA and zeroth-order stochastic models require 25-40 min, while relative errors are of about 3 - 4%. Note that AMF

computation by ISA takes only 1 - 3 min, while the relative errors are below 4%. Figure 1 illustrates the retrieval errors for three synthetic cloudy scenes for 30 and 60 degrees of solar zenith angle.

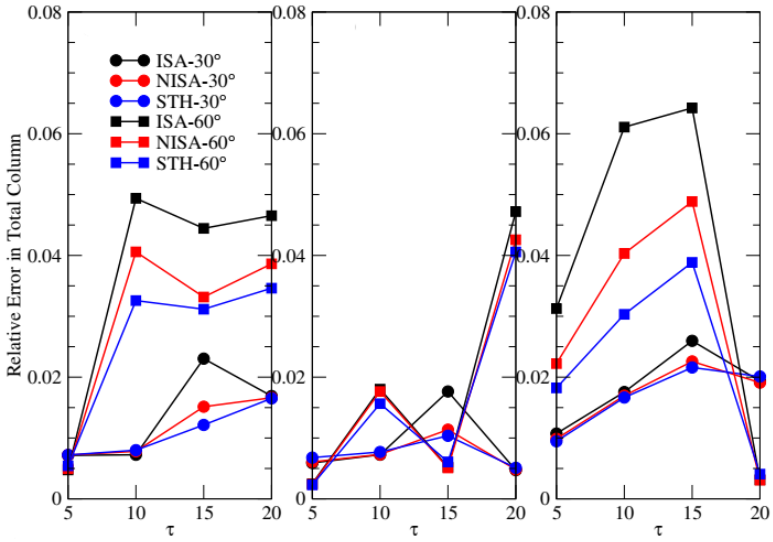

Figure 1. The retrieval errors for three cloudy scenarios using ISA, NISA and stochastic models.

Table 3. Summary of the Radiative Transfer Models.

Name	Description	Features	Pros	Cons	Reference
SHDOM	3D deterministic model	Computes radiance field in 3D geometry	High accuracy	High computation time	Evans, 1998
VSHDOM	3D deterministic model	Computes Stokes parameters in 3D geometry	High accuracy	High computation time	Doicu et al., 2013b
LSHDOM	3D deterministic model	Computes the radiance field in 3D geometry and corresponding derivatives	High accuracy	High computation time	Doicu et al., 2018
ISA	Independent slice approximation (2D)	Computes 2D scene for a single slice of the 3D scene	Faster than 3D computations by order of magnidue	May lead to low accuracy in some scenarious	
NISA	Independent slice approximation (2D)	Computes 2D scene for a set of slices of the 3D scene and then averages them	More accurate than ISA due to better account of the 3D effects	Slower than ISA	
paNTICA	parameterized nonlocal tilted independent column approximation	Uses the independent column approximation in conjunction with	Essentially, 3D computations are substituted with fast multiple	Requires the knowledge of the averaging kernel (not	Wissmeier et al. (2013)

		averaging procedures across the 3D scene	1D computations	available in practice)	
Stochastic model (DLR)	Computes the radiance field and its fluctuations for broken clouds	Uses a deterministic solver	Can take into account the effects of broken clouds at low computational cost	Broken cloud assumption has to be justified. The error of the model as compared to 3D models has unpredicted behavior	Doicu et al, 2014a
Stochastic model (Titov)	Computes the mean radiances in clear sky and inside the cloud	Uses the Monte-Carlo solver	Can take into account the effects of broken clouds at low computational cost	Implementation is not available. The computations of derivatives are not implemented.	Titov, 1990
TICA	1D RTM	Direct and diffuse radiations are calculated in the tilted, independent columns that are slanted according to the solar zenith and azimuth angles	Computationally very fast	The systematic analysis of the accuracy is required	
NTICA	1D RTM	Works as TICA, but accounts for the diffuse radiation transport between the tilted columns by convolving the TICA reflectances with a kernel function.	Computationally very fast	Slower than TICA. The knowledge of the averaging kernel is required.	

3.1.3 3DCTRL Products

3.1.3.1 Synthetic dataset to validate trace gas retrieval algorithms

We will use the same cloud input that was defined for the ESA-3DCATS project: The first set of synthetic data includes a 2D cloud, for which the following cloud parameters will be varied: cloud optical thickness, cloud bottom height, cloud geometrical thickness, and effective radius of cloud droplets/crystals. This setup is very useful to test the sensitivity of the NO_2 retrieval error on solar zenith angle, surface albedo and

various cloud parameters. Corresponding 1D cloudy and clear sky simulations will also be performed to compare 3D RT simulations with the commonly used IPA (Independent Pixel Approximation) approach. The second set of synthetic data includes cloud properties simulated by the LES model ICON for a region covering Germany and parts of surrounding countries with a spatial resolution of approximately 1x1km². In the ESA-3DCATS project it has been shown by comparison with VIIRS observations that the simulated cloud properties from ICON are realistic in a statistical sense (Emde et al. 2022). All cloud types typically found in central Europe such as shallow cumulus, convective cloud cells, cirrus, and stratocumulus are included. The synthetic Sentinel-S5P observations will be simulated at a spatial resolution of 3.5x7km². The cloud input from the ICON model has a spatial resolution of about 1x1km², this means that sub-pixel cloudiness is considered. Representative sun-observer geometries for LEO (S5P, S5) and GEO (S4) orbits will be included. Surface reflection will be treated as Lambertian with various representative surface albedos.

The synthetic dataset will include all bands that are used by the various NO_2 retrieval algorithms including various cloud correction schemes. The BIRA retrieval algorithms (Blond et al., 2007; De Smedt et al., 2008) use band 4 (405-500nm) and the O2A band region, and the synthetic dataset from 3DCATS has already been used to quantify the retrieval error of NO_2 VCD due to 3D cloud scattering (Yu et al 2022, Kylling et al. 2022). The retrieval algorithms OCRA/ROCINN developed by DLR (Loyola et al., 2018, Lutz et al., 2016, Loyola et al., 2007) require in addition band 3 (310-405nm) and a wider region around the O2A-band (758-772nm). Therefore, the synthetic dataset that has been established in the ESA-3DCATS project will be extended by this spectral regions to allow applicability for the trace gas retrieval algorithms developed by DLR.

3.1.3.2 Tropospheric NO_2 columns from synthetic spectra

The tropospheric NO_2 retrieval for synthetic data uses the DOAS method. In DOAS, the AMF, needed to convert SCD to VCD, is calculated using the solar zenith angle, viewing zenith angle, relative azimuth angle, surface albedo, surface pressure, cloud information, NO_2 profile, as well as the pre-calculated layer-AMF LUT, and the layer-AMFs are derived using the VLIDORT RTM. The AMF calculation accounts for cloud-contaminated pixels based on the IPA approach, which is used to express the AMF as a linear combination of a cloudy AMF and a clear-sky AMF. Clouds are treated as a simple model based on radiometric cloud fraction estimates and photon path length corrections based on oxygen collision pair (O_2-O_2) at 477 nm or O_2-A absorption band measurements around 760nm.

The radiative transfer model settings in the NO_2 and cloud retrievals are made as consistent as possible with those used to generate the synthetic data sets. Although some errors are inevitable, such as those related to differences between MYSTIC and VLIDORT RTM, or due to interpolation in the LUTs, these errors are generally small. We therefore confident that the main source of error in the NO_2 retrieval is due to the cloud correction. The error of the NO_2 retrieval is generally evaluated by comparing the calculated AMF with the true AMF, which is computed using the layer-AMFs from MYSTIC

3.1.3.3 Tropospheric NO_2 columns from S5P/TROPOMI spectra

3.2 Validation Datasets

3.2.1 Satellite-based validation datasets

3.2.1.1 Cloud parameter datasets

3.2.1.1.1 TROPOMI Cloud Datasets

For S5P/TROPOMI, several cloud products have been developed that use different physical processes as approaches to retrieve cloud parameters such as cloud fraction, cloud height, and cloud optical thickness.

- The operational cloud retrieval algorithms for TROPOMI were developed by DLR as a two-step algorithm (Loyola et al., 2018, Loyola et al., 2021). The Optical Cloud Recognition Algorithm (OCRA) retrieves the cloud fraction using TROPOMI measurements in the UV and VIS spectral regions

(using TROPOMI bands 3 and 4), and the Retrieval of Cloud Information using Neural Networks (ROCINN) retrieves the cloud top height (pressure) and optical thickness (albedo) using TROPOMI measurements in and around the O_2 A-band in the NIR from 758 to 772 nm (using TROPOMI band 6). Due to the geospatial mis-registration between TROPOMI bands 3/4 and band 6, a co-registration scheme is applied for the operational L2_CLOUD product such that the cloud parameters are provided both for the band 3/4 footprints and for the band 6 footprints.

- The Fast Retrieval Scheme for Clouds from the O_2 A-band (FRESCO) algorithm, developed by KNMI, models the effective cloud fraction and cloud pressure (height) using the O_2 A-band centered at 760nm (Koelemeijer et al., 2001; Wang et al., 2008). The cloud parameters are retrieved from top-of-atmosphere reflectance in three 1-nm wide wavelength windows at 758-759 nm (no absorption), 760-761 nm (strong absorption), and 765-766 nm (moderate absorption).
- The O_2-O_2 algorithm has been developed by KNMI and was originally intended for OMI (Acarreta et al., 2004; Veefkind et al., 2016). The algorithm uses TROPOMI measurements from the O_2-O_2 absorption window at 477 nm to retrieve the effective cloud fraction and the cloud height using a similar cloud model as the one used in FRESCO. Clouds are treated as Lambertian reflectors with a fixed cloud albedo of 0.8.

3.2.1.1.2 VIIRS Cloud Datasets

S5P/TROPOMI does not include an imager for cloud information. However, it flies in tandem with the Suomi National Polar-orbiting Partnership (S-NPP) satellite. The S-NPP payload includes the Visible Infrared Imaging Radiometer Suite (VIIRS) instrument, which may be used as an imager for TROPOMI. The difference in overpass time is slightly more than 4 min, and care must be taken with, for example, the movement of clouds when combining data from the two platforms (Trees et al, 2022). The VIIRS L2 data includes various cloud products such as the cloud mask, cloud shadow, cloud optical thickness, and cloud top height products. Furthermore, VIIRS L1b is used to calculate the H metric which is the standard deviation of VIIRS band reflectances divided by the mean of the VIIRS reflectances within a TROPOMI pixel. It is an estimate of the variation of radiance within the TROPOMI pixel and in the presence of sub-pixel clouds, the H metric is expected to increase as the horizontal cloud inhomogeneity increases. In the absence of clouds, the H metric is expected to be small (Kylling et al, 2022).

The spatial resolution of the VIIRS M-band data used in 3DCTRL is 750x750 m². Thus, VIIRS cloud products may be used to identify clouds smaller than the TROPOMI pixel and to study cloud and cloud shadow fraction effects. The TROPOMI data include the latitude and longitude of the corners of each TROPOMI pixel, and this information is used to identify VIIRS pixels within each TROPOMI pixel.

3.2.1.2 Tropospheric NO_2 columns

3.2.1.2.1 TROPOMI

The operational TROPOMI NO_2 retrieval algorithm was developed by KNMI based on the Dutch OMI NO_2 (DOMINO) retrieval algorithm (Boersma et al., 2011) and several improvements from the Quality Assurance for Essential Climate Variables (QA4ECV) and other projects (Lorente et al., 2017; Boersma et al., 2018; van Geffen 2020, 2022). The NO_2 SCD was retrieved from DOAS fitting over 405-465 nm and then separated into tropospheric and stratospheric parts based on data assimilation in the TM5-MP CTM (Williams et al., 2017). The tropospheric component is converted into the VCD by the AMF. The AMF was calculated based on a look-up table (LUT) of altitude-dependent AMFs and the vertical distribution of NO_2 from the TM5-MP CTM (1°×1° grid; van Geffen et al., 2021). The surface albedo was adopted from OMI climatology (Kleipool et al., 2008), while cloud pressure from the TROPOMI FRESCO product and radiometric cloud fraction from the NO_2 fitting window (around 440 nm) were utilized for the calculation (van Geffen et al., 2021).

3.2.2 Ground-based validation datasets

3.2.2.1 MAX-DOAS tropospheric NO_2 columns

Multi Axis Differential Optical Absorption Spectroscopy (MAX-DOAS) in the atmosphere is a relatively new ground-based passive measurement technique that represents a significant development on the well-established zenith scattered sunlight DOAS instruments, which are mainly sensitive to stratospheric absorbers (Hönninger *et al.*, 2004). MAX-DOAS utilizes scattered sunlight in the ultraviolet (UV) and visible (VIS) parts of the electromagnetic spectrum received from multiple elevation angles, and the recorded spectra are analyzed using DOAS (Platt and Stutz, 2008) for the determination of the differential slant column densities (dSCDs) (Sinreich *et al.*, 2005). The ground-based MAX-DOAS observational technique is highly sensitive to various absorbers, such as NO_2, HCHO, H_2O, BrO, SO_2, etc., in the lowest few kilometers of the atmosphere and vertical profile information can be retrieved from a single elevation sequence (i.e., spectra recorded at different elevation angles that belong to the same azimuthal direction) by combining the measurements with Radiative Transfer Model (RTM) simulations (e.g., Irie *et al.*, 2011). The application of these instruments to air quality observation, monitoring and validation has been immediate and widespread. Different suites of MAX-DOAS instruments have been organized and their datasets homogenized either per geographic location, such as for the Asia Network[1], or per instrumentation make-up and characteristics, such as the BIRA/IASB instruments[2], the Bremen DOAS network[3], the Heidelberg MAX-DOAS instruments[4], etc. MAX-DOAS instruments have also already been incorporated, as highly dependable atmospheric measurements, into international repositories, global projects and official databases, such as the FP7 QA4ECV project[5], the FP7 NORS project[6], the ESA FRM4DOAS project[7], and so on. Highly successful multi-instrumental campaigns have also been organized already by the community, such as the CINDI[8] and CINDI-2 inter-comparison campaigns, the ESA AROMAT and AROMAT-2 campaigns[9], and so on. Within the 3DCTRL project data from MAX-DOAS instruments or Pandora spectrophotometers that systematically report to the ESA Atmospheric Validation Data Centre (EVDC) repository (https://evdc.esa.int/) will be utilized for the evaluation of the improved algorithm for cloud handling and for the validation of the updated S5P tropospheric NO_2 vertical columns (see also section 4.2). Some possible measurement sites that provide ground-based MAX-DOAS NO_2 columns to the EVDC repository and will be used are reference ground-based datasets are listed in Table 4.

Table 4. Description of the ground-based MAX-DOAS NO_2 datasets that will be used for the validation strategy

Institute	Location (lat/lon)	Reference
AUTH	Thessaloniki, Greece (40.63° N, 22.96° E)	Drosoglou et al., 2017; Karagkiozidis et al., 2022
BIRA-IASB	Uccle, Belgium (50.8° N, 4.32° E)	Dimitropoulou et al., 2020, 2021
BIRA-IASB	Xianghe, China (39.75° N, 116.96° E)	Clémer et al., 2010; Hendrick et al., 2014
IUPB	Athens, Greece (38.05° N, 23.86° W)	Gratsea et al., 2021 a, b
IUPB	Bremen, Germany (53.11° N, 8.86° E)	Wittrock et al., 2004
KNMI	Cabauw, the Netherlands (51.971° N, 4.927° E)	Piters et al., 2012
KNMI	De Bilt, the Netherlands (52.101° N, 5.178° E)	Vlemmix et al., 2010, 2015
MPIC	Mainz, Germany (49.99° N, 8.23° E)	Ma et al., 2013; Wang et al., 2017

[1] See https://www.jamstec.go.jp/egcr/e/atmos/observation/topics2.html
[2] See http://uv-vis.aeronomie.be/groundbased/instruments/Instrument.php
[3] See http://www.iup.uni-bremen.de/doas/groundbased_data.htm
[4] See https://www.hce.uni-heidelberg.de/analytics_en/lab_doas_pla.html
[5] See http://www.qa4ecv.eu/
[6] See http://nors.aeronomie.be/index.php
[7] See http://frm4doas.aeronomie.be/
[8] See http://projects.knmi.nl/cindi/
[9] See https://uv-vis.aeronomie.be/news/20141205/ and https://uv-vis.aeronomie.be/news/20150923/

3.2.2.2 Visible all-sky camera

Clouds have a strong influence on the radiative transfer in the atmosphere by absorbing and scattering radiation and hence they affect the analysis of measurements of the solar radiation. Cloud detection, typing and characterization can be performed by scientific equipment that is specifically designed for this work, such as Light Detection And Ranging (LIDAR) systems and ceilometers using zenith-sky observations. However, other instruments (such as MAX-DOAS systems) perform spectral measurements of scattered sunlight at multiple viewing directions (see also section 3.2.2.1) and hence imaging of the whole sky around the measurement site is critical for cloud detection and cloud fraction estimation in order to evaluate the quality of the observation data. A sky-camera is a relatively low-cost equipment, it is easy to install and can provide images of the whole sky dome in a high and adjustable temporal resolution. The Laboratory of Atmospheric Physics, Thessaloniki, Greece (40.63° N, 22.96° E) is a measurement site that hosts a commercial visible all-sky-imaging system since 2012 (Kazadzidis et al., 2012) A fish-eye lens is mounted in front of the camera's entrance optics, allowing for a field of view of 180°. Images of the sky have been captured every 15 min and since 2019 the camera's temporal resolution was set to 1 min. No mechanism for obscuring the direct solar radiation is used and thus both the sun disk and the circumsolar light are visible in all images during cloud-free conditions. The camera is adjusted to acquire images that are stored in 24-bit JPEG format with a resolution of 1280×960 pixels. Within the 3DCTRL project the sky-camera can be a useful tool for the determination of the cloud conditions for selected interesting cases, where the retrieval algorithm for 3D cloudy scenes will be evaluated.

4. Validation Strategy

4.1 Evaluation of the retrieval algorithm for 3D cloudy scenes

Prior to the comparison of the updated tropospheric NO_2 S5P TROPOMI product with the current operational product and its validation with reference ground-based datasets, the retrieval algorithm for 3D cloudy scenes needs to be evaluated. The algorithm evaluation will be performed using both synthetic and real S5P/TROPOMI observations. Thus, certain representative test cases, where the cloud coverage is clearly distinguishable, need to be identified and especially cases that are characterized by high tropospheric NO_2 content will be investigated, taking also into account the availability of reference ground-based trace gas concentration and ancillary cloud coverage data. LAP/AUTH is a potential location for the evaluation of the algorithm since monitoring of trace gases (including NO_2) in the troposphere is routinely performed by multiple MAX-DOAS instruments, whose time series cover the whole time period that TROPOMI operates, and it also hosts a sky-camera that provides continuous information about the cloud fraction around the measurement site in a high temporal resolution. Figure 2 shows some sample images captured by the sky-camera at LAP/AUTH under different cloud conditions (clear-sky, broken clouds, overcast), where the cloud coverage is clearly distinguishable.

Figure 2. Sample images captured the sky-camera at LAP/AUTH under different cloud conditions (left: clear-sky; middle: broken clouds; right: overcast). Numerous collocated ground-based and satellite data are available since the sky-camera stores an image of the whole sky every 1 minute (hence also during S5P overpasses) and therefore the time difference between the two instruments would be negligible. High NO_2 concentration levels are not infrequent at LAP/AUTH, especially during the cold period. The synergy of the sky-camera and the MAX-DOAS systems will make available the identification of the required highly NO_2 polluted cases under different cloud conditions, that are mentioned above, for the evaluation of the improved algorithm for 3D cloud handling.

For the test cases the S5P/TROPOMI cloud products will be compared with corresponding VIIRS cloud products. Furthermore, it will be investigated how TROPOMI sub-pixel cloud inhomogeneities affect the S5P/TROPOMI cloud products. TROPOMI sub-pixel information will be derived both from VIIRS cloud information and from the ground-based LAP/AUTH all sky camera for the test cases.

4.2 Validation of the updated tropospheric NO_2 S5P/TROPOMI product

Within the 3DCTRL project the S5P tropospheric NO_2 vertical columns will be evaluated and validated using data from multiple ground-based MAX-DOAS instruments or Pandora spectrophotometers, that are distributed mainly around Europe and Asia (see also Table 4) and they report to the EVDC repository. The validation will be performed in both heavily polluted urban environments, such as in Xianghe, China in the outskirts of Beijing, and also in less polluted urban locations, e.g., in Athens and Thessaloniki, Greece. Thus, the operational S5P/TROPOMI tropospheric NO_2 product and the optimized product will be compared under various NO_2 concentration levels. Collocated measurements between the satellite and the ground-based instruments will be found and the validation will be performed in terms of both daily and monthly mean values. The effect of various known geophysical parameters (such as the Solar Zenith Angle, the distance of the S5P pixel from the overpass location and the ground-based azimuth viewing direction) on the retrieved columns will be investigated. The comparison between the satellite and the ground-based product will be conducted for all seasons in order to investigate their seasonal variability and to evaluate their performance under both low and high NO_2 concentration levels. The current status of the S5P/TROPOMI tropospheric NO_2 product (for LAP/AUTH only) is presented in Figure 3 and Figure 4. The timeseries of the collocated ground-based and TROPOMI's NO_2 vertical column measurements is presented in Figure 2 in box-and-whisker plots, while the direct comparison between the ground-based and the satellite-derived product is

presented in a scatter plot in Figure 3 for the period May 2020 to March 2022. Higher variability for both MAX-DOAS and S5P/TROPOMI NO_2 observations are seen during winter-time. This is to be expected since NOx emissions sources are higher during winter-time, which, combined with the lower photolysis rate of NO2 due to limited sunlight and the higher variable weather patterns, results in higher spatio-temporal variability in both sources of observation. Overall, TROPOMI systematically reports lower NO_2 columns than the MAX-DOAS. The underestimation of satellite-derived tropospheric NO_2 compared to the MAX-DOAS is also found in recent publications (e.g., Griffin et al., 2019; Pinardi et al., 2020; Dimitropoulou et al., 2020) and it is more evident in highly polluted and in extremely highly polluted environments (Verhoelst et al., 2021). The MAX-DOAS probes air masses along the line of sight of the telescope, pointing at different elevation angles, from near the horizon to the zenith. The measurements are sensitive to local emissions located on this line of sight and at distances up to ~10 km. The NO_2 columns that are reported by satellite instruments are essentially averaged over the sub-satellite pixel area (3.5 x 5.5 km² for S5P/TROPOMI) which contain different emissions sources, resulting, generally, to underestimation of the NO_2 columns. Currently, the recommendation for the S5P/TROPOMI tropospheric NO_2 product is to cut-off measurements where the cloud fraction is greater than 20% in order to obtain a higher quality product. This filtering, however, rejects a large fraction of the available data, especially at locations where clear-sky conditions are not so frequent. The collocations with the MAX-DOAS measurements are even fewer, making the comparison and validation of the S5P product less robust. The availability of an updated satellite NO_2 product of higher quality under cloudy scenes will provide the capability of a further in depth validation of TROPOMI NO_2 columns and its performance in various locations around the globe under different NO_2 concentration levels.

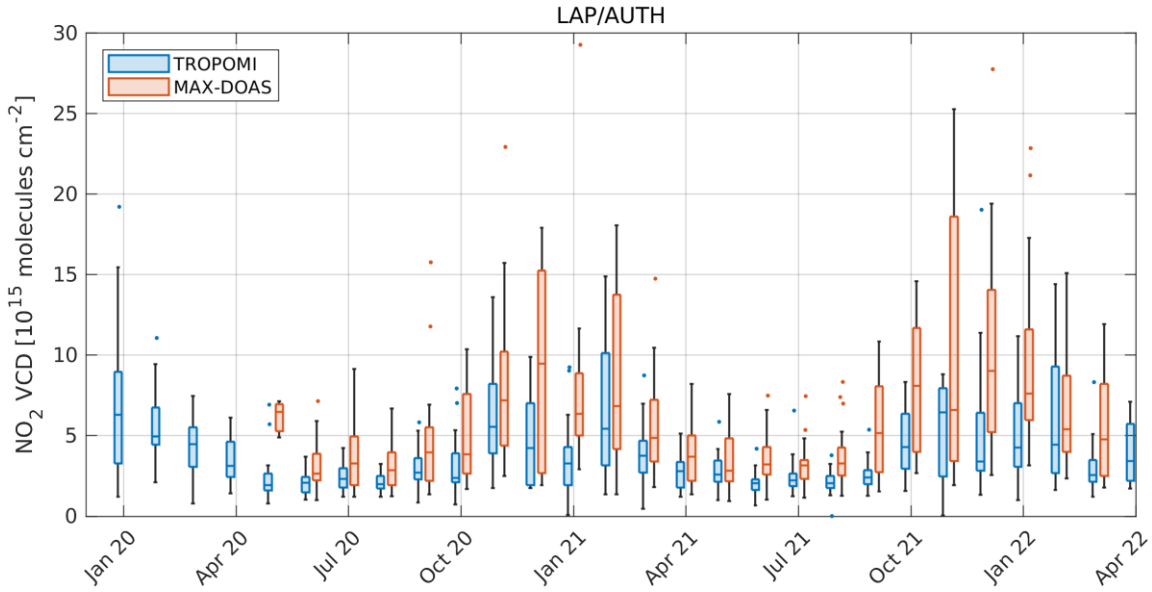

Figure 3. Monthly mean timeseries of the collocated ground-based MAX-DOAS and S5P/TROPOMI tropospheric NO_2 vertical columns at LAP/AUTH for the period May 2020 to March 2022.

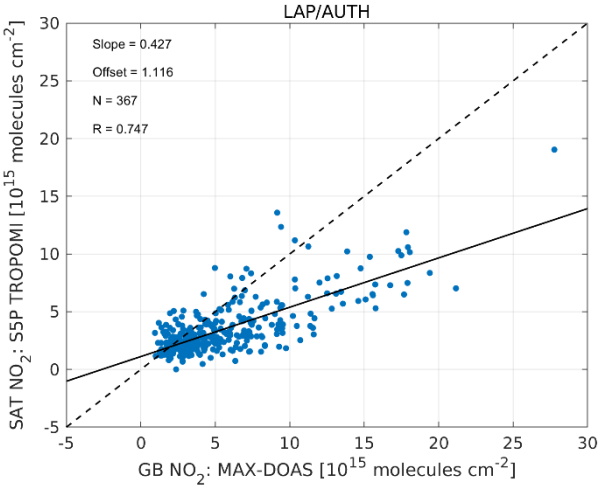

Figure 4. Scatter plot of the daily collocated tropospheric NO_2 VCDs that are reported by the MAX-DOAS and S5P/TROPOMI.

5. Scientific and Dataset Requirements

This section describes the scientific requirements of the planned work as well as the foreseen input data, output data fields and proposed output data format.

5.1 Scientific Requirements

The requirements for the tropospheric NO_2 column bias and random error are 20-50% and $0.7x10^{15}$ molecules/cm^2, respectively, on a pixel level (van Geffen et al., 2019). The ESA-funded 3DCATS project showed that 3D cloud effects may result in NO_2 column density bias on the order of tens of % for solar zenith angles larger than about 40 degrees. The 3DCTRL project aims to reduce the uncertainty in the tropospheric vertical column due to the treatment of 3D clouds.

5.2 Dataset Requirements

5.2.1 Input data

We note here is a first collection of potential input data which might be extended during the project.

Table 5 Input data for the 3DCTRL algorithms

<table>
<tr><th>Name / Data</th><th>Source</th><th>Remarks</th></tr>
<tr><td>Earth radiance</td><td>S5p L1b product (BD3)</td><td></td></tr>
<tr><td>Sun irradiance</td><td>S5p L1b product (IRR)</td><td></td></tr>
<tr><td>Viewing geometry</td><td></td><td rowspan="11">Dataset available in S5p L2 NO_2 product</td></tr>
<tr><td>NO_2 VCD</td><td rowspan="3">S5p operational NO_2 product</td></tr>
<tr><td>NO_2 AMF</td></tr>
<tr><td></td></tr>
<tr><td>Cloud fraction</td><td rowspan="3">S5p operational cloud product based on a Lambertian cloud model (CRB)</td></tr>
<tr><td>Cloud top pressure</td></tr>
<tr><td>Cloud top albedo</td></tr>
<tr><td>Surface pressure</td><td rowspan="2">S5p operational cloud product</td></tr>
<tr><td>Surface albedo</td></tr>
<tr><td>Cloud shadow</td><td>VIIRS L2 product</td></tr>
<tr><td>Cloud shadow fraction</td><td>Calculated from cloud shadow</td><td></td></tr>
<tr><td>Cloud mask</td><td>VIIRS L2 product</td><td></td></tr>
<tr><td>Cloud fractions</td><td>Calculated from cloud mask and VIIRS L1b radiances</td><td></td></tr>
<tr><td>Cloud top height</td><td>VIIRS L2 product</td><td></td></tr>
<tr><td>Cloud liquid water content (3D)</td><td>ICON LES model</td><td></td></tr>
<tr><td>Cloud ice water content (3D)</td><td>ICON LES model</td><td></td></tr>
</table>

5.2.2 Output data & format

5.2.2.1 Synthetic dataset for validation of retrieval algorithms

The synthetic data defined in Section 3.1.1.4 will be generated for the spectral bands given in Table 8. All spectra will be simulated for the input settings summarized in Table 6 (2D clouds) and Table 7 (LES clouds).

Table 6. Input settings for synthetic dataset with 2D cloud

	Liquid water cloud	Ice water cloud
Cloud optical thickness	1, 2, 5, 10, 20	1, 2, 5, 10, 20
Cloud bottom height [km]	2, 5, 10	5, 9, 12
Effective radius [µm]	10	30
Optical properties	Mie	Baum (V3.6)
Cloud geometrical thickness [km]	0.2, 1, 2, 4, 8	
Surface albedo	0.02, 0.05, 0.1, 0.15, 0.2, 0.3	
Solar zenith angle [deg]	20, 30, 40, 50, 60, 70, 80	

Table 7. Representative sun positions, sensor viewing directions and surface albedos included in the synthetic dataset with 3D cloud input data from LES model.

	Geostationary orbit	Low Earth orbit
Solar zenith angles [deg]	20, 40, 60	20, 40, 60
Solar azimuth angles [deg]	−90, -45, 0, 45, 90	13, 353
Sensor viewing zenith angle [deg]	58,3	0, 20, 60
Sensor viewing azimuth angle [deg]	196,3	109.5, 281.7
Surface albedo	0, 0.05, 0.2 (0.5 for O2A-band)	

Table 8. Spectral bands included in the synthetic TROPOMI-S5P dataset

Synthetic observation	Spectral range	Spectral resolution	Remarks
UV reflectance (band 3)	310-405 nm	0.2 nm	not yet available
VIS reflectance (band 4)	405-500 nm	0.2 nm	available from 3DCATS
O2A-band reflectance	758-772nm	0.005 nm	partly available from 3DCATS, spectral range to be extended

The synthetic dataset will be stored in netcdf-format and provided along with detailed documentation on the project website. Also, the software (PYTHON, SLURM) that will be developed to run the radiative transfer simulations on the MIM cluster will be provided.

Table 9 Suggested output of the 3DCTRL NO_2 products

Variable	Unit	L2 variable name	Dimension
NO_2 total column	mol/cm^2	*total_nitrogen_dioxide_vertical_column*	nGround x nScan
NO_2 tropospheric column	mol/cm^2	*tropospheric_nitrogen_dioxide_vertical_column*	nGround x nScan

NO_2 total column precision	mol/cm^2	*total_nitrogen_dioxide_vertical_column_precision*	nGround x nScan
NO_2 tropospheric column precision	mol/cm^2	*tropospheric_nitrogen_dioxide_vertical_column_precision*	nGround x nScan
Cloud parameters			nGround x nScan

6. Risk Analysis

In this section a consolidated risk analysis is provided pointing out which risk areas could affect the final success of the project and the proposed solutions. By nature, research & innovation projects like the 3DCTRL project have to be effectively organized in order to handle unforeseen outcomes, since their future is less predictable than for e.g. operational activities. To this end, the objective of risk analysis and management is to provide the process and techniques for the evaluation and control of potential project risks, focusing on their precautionary diagnosis and handling. There are inherent risks related to situations external to the project and risks related to internal consortium problems; thus, the risk management process involves two activities: (a) Risk Analysis: identification of a risk and assessment of its importance and evaluation of whether the risk level is acceptable for the project; (b) Risk Management: planning of required activities to handle the risk, redistribution of resources, evaluation of the results and ensuring that the new status is stable enough. A list of potential risks has been identified and is described together with the contingency in Table 10.

Table 10 Risk, type, related impact and probability of occurrence and proposed solution.

Risk	Impact	Type	Probability	Proposed solution(s)
Overall accuracy requirements not met.	Major. This is the main aim of this project.	Compliance	Minor.	Identify the possible causes and report them for future advancement in the field.
Accuracy requirements for specific types of clouds.	Medium. This is part of the aims of this project.	Compliance	Medium.	Identify the possible causes and report them for future advancement in the field.
Project timeline requirements not met.	Major.	Strategic	Minor	Internal re-distribution of resources, mobilization of another consortium member into the WP in delay.
Lack of sufficient verification datasets.	Major, since verification cannot be performed adequately.	Operational	Minor	Select ab initio validation test areas where validation datasets exist.
Lack of accuracy/precision information of the verification datasets.	Medium, since the verification will not be rendered valid.	Operational	Medium	Perform a statistical analysis on the dependability of the verification datasets based on literature.

Bibliography

Acarreta, J. R., De Haan, J. F., and Stammes, P.: Cloud pressure retrieval using the O_2-O_2 absorption band at 477 nm, J. Geophys. Res., 109, D05 204, https://doi.org/10.1029/2003JD003915, 2004.

Alexandrov, M.; Marshak, A.; Ackerman, A. Cellular Statistical Models of Broken Cloud Fields. Part I: Theory. J. Atmos. Sci. 2010, 67, 2125–2151.

Anderson, G., Clough, S., Kneizys, F., Chetwynd, J., and Shettle, E.: AFGL atmospheric constituent profiles (0-120 km), Tech. Rep. AFGL-TR-86-0110, Air Force Geophys. Lab., Hanscom Air Force Base, Bedford, Mass., 1986.

Baum, B. A., Yang, P., Heymsfield, A. J., Bansemer, A., Merrelli, A., Schmitt, C., and Wang, C.: Ice cloud bulk single-scattering property models with the full phase matrix at wavelengths from 0.2 to 100 μm, J. Quant. Spectrosc. Radiat. Transfer, 2014

Blond, N., Boersma, K. F., Eskes, H. J., van der A, R. J., Van Roozendael, M., De Smedt, I., Bergametti, G., and Vautard, R.: Intercomparison of SCIAMACHY nitrogen dioxide observations, in situ measurements and air quality modeling results over Western Europe, Journal of Geophysical Research: Atmospheres, 112, https://doi.org/10.1029/2006JD007277, 2007.

Boersma, K. F., Eskes, H. J., Dirksen, R. J., van der A, R. J., Veefkind, J. P., Stammes, P., Huijnen, V., Kleipool, Q. L., Sneep, M., Claas, J., Leitão, J., Richter, A., Zhou, Y., and Brunner, D.: An improved tropospheric NO_2 column retrieval algorithm for the Ozone Monitoring Instrument, Atmos. Meas. Tech., 4, 1905–1928, https://doi.org/10.5194/amt-4-1905-2011, 2011.

Boersma, K. F., Eskes, H. J., Richter, A., De Smedt, I., Lorente, A., Beirle, S., van Geffen, J. H. G. M., Zara, M., Peters, E., Van Roozendael, M., Wagner, T., Maasakkers, J. D., van der A, R. J., Nightingale, J., De Rudder, A., Irie, H., Pinardi, G., Lambert, J.-C., and Compernolle, S. C.: Improving algorithms and uncertainty estimates for satellite NO_2 retrievals: results from the quality assurance for the essential climate variables (QA4ECV) project, Atmos. Meas. Tech., 11, 6651–6678, https://doi.org/10.5194/amt-11-6651-2018, 2018.

Clémer, K., Van Roozendael, M., Fayt, C., Hendrick, F., Hermans, C., Pinardi, G., Spurr, R., Wang, P., and De Mazière, M.: Multiple wavelength retrieval of tropospheric aerosol optical properties from MAXDOAS measurements in Beijing, Atmos. Meas. Tech., 3, 863–878, https://doi.org/10.5194/amt-3-863-2010, 2010.

De Smedt, I., Müller, J.-F., Stavrakou, T., van der A, R., Eskes, H., and Van Roozendael, M.: Twelve years of global observations of formaldehyde in the troposphere using GOME and SCIAMACHY sensors, Atmospheric Chemistry and Physics, 8, 4947–4963, https://doi.org/10.5194/acp-8-4947-2008, https://www.atmos-chem-phys.net/8/4947/2008/, 2008.

Dimitropoulou, E., Hendrick, F., Friedrich, M. M., Tack, F., Pinardi, G., Merlaud, A., Fayt, C., Hermans, C., Fierens, F., and Van Roozendael, M.: Horizontal distribution of tropospheric NO_2 and aerosols derived by dual-scan multi-wavelength MAX-DOAS measurements in Uccle, Belgium, Atmos. Meas. Tech. Discuss. [preprint], https://doi.org/10.5194/amt-2021-308, in review, 2021.

Dimitropoulou, E., Hendrick, F., Pinardi, G., Friedrich, M. M., Merlaud, A., Tack, F., De Longueville, H., Fayt, C., Hermans, C., Laffineur, Q., Fierens, F., and Van Roozendael, M.: Validation of TROPOMI tropospheric NO_2 columns using dual-scan multi-axis differential optical absorption spectroscopy (MAX-DOAS) measurements in Uccle, Brussels, Atmos. Meas. Tech., 13, 5165–5191, https://doi.org/10.5194/amt-13-5165-2020, 2020.

Dipankar, A., Stevens, B., Heinze, R., Moseley, C., Zängl, G., Giorgetta, M., and Brdar, S.: Large eddy simulation using the general circulation model ICON, Journal of Advances in Modeling Earth Systems, 7, 963–986, https://doi.org/10.1002/2015MS000431,2015.

Doicu A., Efremenko D., 2019. Linearizations of the Spherical Harmonic Discrete Ordinate Method (SHDOM). Atmosphere, 10, 292.

Doicu A., Efremenko D., Trautmann T, 2013a. An analysis of the short-characteristic method for the spherical harmonic discrete ordinate method (SHDOM). J. Quant. Spectrosc. Radiat. Transf., 119, 114–127.

Doicu A., Efremenko D., Trautmann T., 2013b. A multi-dimensional vector spherical harmonics discrete ordinate method for atmospheric radiative transfer. J. Quant. Spectrosc. Radiat. Transf. Journal, 118, 121-131.

Doicu A., Efremenko D., Trautmann T., 2020a. A Spectral Acceleration Approach for the Spherical Harmonics Discrete Ordinate Method. Remote Sens., 12, 3703.

Doicu A., Efremenko D.S., Loyola D., Trautmann T., 2014a. Discrete ordinate method with matrix exponential for stochastic radiative transfer in broken clouds. J. Quant. Spectrosc. Radiat. Transfer,138, 1-16

Doicu A., Efremenko D.S., Loyola D., Trautmann T., 2014b. Approximate models for broken clouds in stochastic radiative transfer theory. J. Quant. Spectrosc. Radiat. Transfer, 145, 74-87.

Doicu A., Efremenko D.S., Trautmann T., 2021. A Proof-of-Concept Algorithm for the Retrieval of Total Column Amount of Trace Gases in a Multi-Dimensional Atmosphere. Remote Sens., 13, 270. https://doi.org/10.3390/rs13020270

Doicu A., Mishchenko M.I., Efremenko D., Trautmann T., 2020b. Spectral Spherical Harmonics Discrete Ordinate Method. J. Quant. Spectrosc. Radiat. Transfer, 258, 107386. doi:10.1016/j.jqsrt.2020.107386

Doicu A., Trautmann T., Schreier F, 2010. Numerical Regularization for Atmospheric Inverse Problems; Springer: Berlin/Heidelberg, Germany.

Drosoglou, T., Bais, A. F., Zyrichidou, I., Kouremeti, N., Poupkou, A., Liora, N., Giannaros, C., Koukouli, M. E., Balis, D., and Melas, D.: Comparisons of ground-based tropospheric NO_2 MAX-DOAS measurements to satellite observations with the aid of an air quality model over the Thessaloniki area, Greece, Atmos. Chem. Phys., 17, 5829–5849, https://doi.org/10.5194/acp-17-5829-2017, 2017.

Efremenko D.S., Doicu A., Loyola D., Trautmann T., 2018: Fast stochastic radiative transfer models for trace gas and cloud property retrievals under cloudy conditions, in Springer Series in Light Scattering: Volume 1: Multiple Light Scattering, Radiative Transfer and Remote Sensing, edited by A. Kokhanovsky. 231-277.

Efremenko D.S., Schüssler O., Doicu A., Loyola D., 2016: A stochastic cloud model for cloud and ozone retrievals from UV measurements, Journal of Quantitative Spectroscopy and Radiative Transfer, 184, 167-179

Emde, C., R. Buras, R., and B. Mayer. ALIS: An efficient method to compute high spectral resolution polarized solar radiances using the Monte Carlo approach. J. Quant. Spectrosc. Radiat. Transfer, 112, 1622-1631, 2011

Emde, C., R. Buras-Schnell, A. Kylling, B. Mayer, J. Gasteiger, U. Hamann, J. Kylling, B. Richter, C. Pause, T. Dowling, and L. Bugliaro. The libradtran software package for radiative transfer calculations (version 2.0.1). Geoscientific Model Development, 9(5):1647-1672, 2016

Emde, C., H. Yu, A. Kylling, M. van Roozendael, K. Stebel, B. Veihelmann, and B. Mayer. Impact of 3D cloud structures on the atmospheric trace gas products from UV-Vis sounders - Part 1: Synthetic dataset for validation of trace gas retrieval algorithms. *Atmospheric Measurement Techniques*, 15(5):1587-1608, 2022.

Evans K.F., 1998: The spherical harmonic discrete ordinate method for three-dimensional atmospheric radiative transfer. J. Atmos. Sci., 55(3):429–446

Gabriel, P. M., and K. F. Evans, 1996: Simple radiative transfer methods for calculating domain-averaged solar fluxes in inhomogeneous clouds. *J. Atmos. Sci.*, **53**, 858–877.

Gasteiger, J., C. Emde, B. Mayer, R. Buras, S.A. Buehler, and O. Lemke. Representative wavelengths absorption parameterization applied to satellite channels and spectral bands. J. Quant. Spectrosc. Radiat. Transfer, 148(0):99-115, 2014

Gratsea, M., Bösch, T., Kokkalis, P., Richter, A., Vrekoussis, M., Kazadzis, S., Tsekeri, A., Papayannis, A., Mylonaki, M., Amiridis, V., Mihalopoulos, N., and Gerasopoulos, E.: Retrieval and evaluation of tropospheric-aerosol extinction profiles using multi-axis differential optical absorption spectroscopy (MAX-DOAS) measurements over Athens, Greece, Atmos. Meas. Tech., 14, 749–767, https://doi.org/10.5194/amt-14-749-2021, 2021.

Gratsea, M.; Athanasopoulou, E.; Kakouri, A.; Richter, A.; Seyler, A.; Gerasopoulos, E. Five Years of Spatially Resolved Ground-Based MAX-DOAS Measurements of Nitrogen Dioxide in the Urban Area of Athens: Synergies with In Situ Measurements and Model Simulations. Atmosphere 2021, 12, 1634. https://doi.org/10.3390/atmos12121634

Griffin, D., Zhao, X., McLinden, C. A., Boersma, F., Bourassa, A., Dammers, E., Degenstein, D., Eskes, H., Fehr, L., Fioletov, V., Hayden, K., Kharol, S. K., Li, S.-M., Makar, P., Martin, R. V., Mihele, C., Mittermeier, R. L., Krotkov, N., Sneep, M., Lamsal, L. N., Linden, M. T., Geffen, J. V., Veefkind, P., and Wolde, M.: High-Resolution Mapping of Nitrogen Dioxide With TROPOMI: First Results and Validation Over the Canadian Oil Sands, Geophys. Res. Lett., 46, 1049–1060, https://doi.org/10.1029/2018GL081095, 2019.

Heinze, R., Dipankar, A., Henken, C. C., Moseley, C., Sourdeval, O., Trömel, S., Xie, X., Adamidis, P., Ament, F., Baars, H., Barthlott, C., Behrendt, A., Blahak, U., Bley, S., Brdar, S., Brueck, M., Crewell, S., Deneke, H., Di Girolamo, P., Evaristo, R., Fischer, J., Frank, C., Friederichs, P., Göcke, T., Gorges, K., Hande, L., Hanke, M., Hansen, A., Hege, H.-C., Hoose, C., Jahns, T., Kalthoff, N., Klocke, D., Kneifel, S., Knippertz, P., Kuhn, A., van Laar, T., Macke, A., Maurer, V., Mayer, B., Meyer, C. I., Muppa, S. K., Neggers, R. A. J., Orlandi, E., Pantillon, F., Pospichal, B., Röber, N., Scheck, L. Seifert, A., Seifert, P., Senf, F., Siligam, P., Simmer, C., Steinke, S., Stevens, B., Wapler, K., Weniger, M., Wulfmeyer, V., Zängl, G., Zhang, D., and Quaas, J.: Large-eddy simulations over Germany using ICON: a comprehensive evaluation, Quarterly Journal of the Royal Meteorological Society, 143, 69–100, https://doi.org/10.1002/qj.2947, 2017.

Hendrick F., G. Pinardi, E. Peters, et al., 2018: QA4ECV HCHO and NO_2 MAXDOAS reference data sets: Product description, available at : uv-vis.aeronomie.be/groundbased/ QA4ECV_MAXDOAS, last access: 17/05/2018.

Hendrick, F., Müller, J.-F., Clémer, K., Wang, P., De Mazière, M., Fayt, C., Gielen, C., Hermans, C., Ma, J. Z., Pinardi, G., Stavrakou, T., Vlemmix, T., and Van Roozendael, M.: Four years of ground-based MAX-DOAS observations of HONO and NO_2 in the Beijing area, Atmos. Chem. Phys., 14, 765–781, https://doi.org/10.5194/acp-14-765-2014, 2014.

Hönninger, G., von Friedeburg, C., and Platt, U.: Multi axis differential optical absorption spectroscopy (MAX-DOAS), Atmos. Chem. Phys., 4, 231–254, https://doi.org/10.5194/acp-4-231-2004, 2004

Irie, H., Takashima, H., Kanaya, Y., Boersma, K. F., Gast, L., Wittrock, F., Brunner, D., Zhou, Y., and Van Roozendael, M.: Eight-component retrievals from ground-based MAXDOAS observations, Atmos. Meas. Tech., 4, 1027–1044, https://doi.org/10.5194/amt-4-1027-2011, 2011.

Karagkiozidis, D., Friedrich, M. M., Beirle, S., Bais, A., Hendrick, F., Voudouri, K. A., Fountoulakis, I., Karanikolas, A., Tzoumaka, P., Van Roozendael, M., Balis, D., and Wagner, T.: Retrieval of tropospheric aerosol, NO_2, and HCHO vertical profiles from MAX-DOAS observations over Thessaloniki, Greece: intercomparison and validation of two inversion algorithms, Atmos. Meas. Tech., 15, 1269–1301, https://doi.org/10.5194/amt-15-1269-2022, 2022.

Kazantzidis, A., Tzoumanikas, P., Bais, A., Fotopoulos, S., Economou, G., 2012. Cloud detection and classification with the use of whole-sky ground-based images. Atmos. Res. 113, 80–88, http://www.sciencedirect.com/science/article/pii/S0169809512001342

King, M. D., S. Platnick, P. Yang, G. T. Arnold, M. A. Gray, J. C. Riédi, S. A. Ackerman, and K. N. Liou, 2004: Remote sensing of liquid water and ice cloud optical thickness and effective radius in the arctic: Application of airborne multispectral MAS data. J. Atmos.Oceanic Technol. 21, 857-875.

Kleipool, Q. L., M. R. Dobber, J. F. de Haan, and P. F. Levelt, Earth surface reflectance climatology from 3 years ofOMI data,J. Geophys. Res.,113, D18308, doi:10.1029/2008JD010290, 2008

Koelemeijer, R. B. A., Stammes, P., Hovenier, J. W. and de Haan J. F.: A fast method for retrieval of cloud parameters using oxygen A-band measurements from Global Ozone Monitoring Experiment, J. Geophys. Res., 106, 3475–3490, https://doi.org/10.1029/2003JD003962, 2001.

Kylling, A., Emde, C., Yu, H., van Roozendael, M., Stebel, K., and Mayer, B., Impact of 3D Cloud Structures on the Atmospheric Trace Gas Products from UV-VIS Sounders Final Report, ESA Contract No. 4000124890/18/NL/FF/gp, 2020.

Kylling, A., Emde, C., Yu, H., van Roozendael, M., Stebel, K., Veihelmann, B., and Mayer, B.: Impact of 3D cloud structures on the atmospheric trace gas products from UV–Vis sounders – Part 3: Bias estimate using synthetic and observational data, Atmos. Meas. Tech., 15, 3481–3495, https://doi.org/10.5194/amt-15-3481-2022, 2022.

Lorente, A., Folkert Boersma, K., Yu, H., Dörner, S., Hilboll, A., Richter, A., Liu, M., Lamsal, L. N., Barkley, M., De Smedt, I., Van Roozendael, M., Wang, Y., Wagner, T., Beirle, S., Lin, J.-T., Krotkov, N., Stammes, P., Wang, P., Eskes, H. J., and Krol, M.: Structural uncertainty in air mass factor calculation for NO_2 and HCHO satellite retrievals, Atmos. Meas. Tech., 10, 759–782, https://doi.org/10.5194/amt-10-759-2017, 2017.

Loyola D. G., García S. G., Lutz R., Argyrouli A., Romahn F., Spurr R. J., Pedergnana M., Doicu A., García V. M., and Schüssler O., 2018: The operational cloud retrieval algorithms from TROPOMI on board Sentinel-5 Precursor, Atmos. Meas. Tech., 11, 409.

Loyola D., Thomas W., Livschitz Y., Ruppert T., Albert P., and Hollmann R., 2007: Cloud properties derived from GOME/ERS-2 backscatter data for trace gas retrieval, IEEE T. Geosci. Remote, 45, 2747–2758

Loyola, D. G., Gimeno García, S., Lutz, R., Argyrouli, A., Romahn, F., Spurr, R. J. D., Pedergnana, M., Doicu, A., Molina García, V., and Schüssler, O.: The operational cloud retrieval algorithms from TROPOMI on board Sentinel-5 Precursor, Atmos. Meas. Tech., 11, 409–427, https://doi.org/10.5194/amt-11-409-2018, 2018.

Loyola, D. G., Lutz, R., Argyrouli, A., and Spurr, R.: S5P/TROPOMI ATBD Cloud Products, Tech. Rep. S5P-DLR-L2-ATBD-400I, issue 2.3, 2021-06-25, German Aerospace Center (DLR), https://sentinel.esa.int/documents/247904/2476257/Sentinel-5P-TROPOMI-ATBD-Clouds, 2021.

Spurr, R. J. D., Kurosu, T. P., and Chance, K. V.: A linearized discrete ordinate radiative transfer model for atmospheric remotesensing retrieval, J. Quant. Spectrosc. Ra., 68, 689–735, 2001.

Lutz, R., Loyola, D., Gimeno García, S., and Romahn, F., 2016: OCRA radiometric cloud fractions for GOME-2 on MetOp-A/B, Atmos. Meas. Tech., 9, 2357–2379.

Ma, J. Z., Beirle, S., Jin, J. L., Shaiganfar, R., Yan, P., and Wagner, T.: Tropospheric NO_2 vertical column densities over Beijing: results of the first three years of ground-based MAX-DOAS measurements (2008–2011) and satellite validation, Atmos. Chem. Phys., 13, 1547–1567, https://doi.org/10.5194/acp-13-1547-2013, 2013.

Mayer, B.: Radiative transfer in the cloudy atmosphere, European Physical Journal Conferences, 1, 75–99, 2009.

Mayer, B. and A. Kylling. Technical note: The libRadtran software package for radiative transfer calculations - description and examples of use. Atmos. Chem. Phys., 5: 1855-1877, 2005

Pinardi, G., Van Roozendael, M., Hendrick, F., Theys, N., Abuhassan, N., Bais, A., Boersma, F., Cede, A., Chong, J., Donner, S., Drosoglou, T., Dzhola, A., Eskes, H., Frieß, U., Granville, J., Herman, J. R., Holla, R., Hovila, J., Irie, H., Kanaya, Y., Karagkiozidis, D., Kouremeti, N., Lambert, J.-C., Ma, J., Peters, E., Piters, A., Postylyakov, O., Richter, A., Remmers, J., Takashima, H., Tiefengraber, M., Valks, P., Vlemmix, T., Wagner, T., and Wittrock, F.: Validation of tropospheric NO_2 column measurements of GOME-2A and OMI using MAX-DOAS and direct sun network observations, Atmos. Meas. Tech., 13, 6141–6174, https://doi.org/10.5194/amt-13-6141-2020, 2020.

Piters, A. J. M., Boersma, K. F., Kroon, M., Hains, J. C., Van Roozendael, M., Wittrock, F., Abuhassan, N., Adams, C., Akrami, M., Allaart, M. A. F., Apituley, A., Beirle, S., Bergwerff, J. B., Berkhout, A. J. C., Brunner, D., Cede, A., Chong, J., Clémer, K., Fayt, C., Frieß, U., Gast, L. F. L., Gil-Ojeda, M., Goutail, F., Graves, R., Griesfeller, A., Großmann, K., Hemerijckx, G., Hendrick, F., Henzing, B., Herman, J., Hermans, C., Hoexum, M., van der Hoff, G. R., Irie, H., Johnston, P. V., Kanaya, Y., Kim, Y. J., Klein Baltink, H., Kreher, K., de Leeuw, G., Leigh, R., Merlaud, A., Moerman, M. M., Monks, P. S., Mount, G. H., Navarro-Comas, M., Oetjen, H., Pazmino, A., Perez-Camacho, M., Peters, E., du Piesanie, A., Pinardi, G., Puentedura, O., Richter, A., Roscoe, H. K., Schönhardt, A., Schwarzenbach, B., Shaiganfar, R., Sluis, W., Spinei, E., Stolk, A. P., Strong, K., Swart, D. P. J., Takashima, H., Vlemmix, T., Vrekoussis, M., Wagner, T., Whyte, C., Wilson, K. M., Yela, M., Yilmaz, S., Zieger, P., and Zhou, Y.: The Cabauw Intercomparison campaign for Nitrogen Dioxide measuring Instruments (CINDI): design, execution, and early results, Atmos. Meas. Tech., 5, 457–485, https://doi.org/10.5194/amt-5-457-2012, 2012

Platt, U. and Stutz, J.: Differential Optical Absorption Spectroscopy, Springer-Verlag Berlin Heidelberg, https://doi.org/10.1007/978-3-540-75776-4, 2008

Pomraning G.C. A model for interface intensities in stochastic particle transport // J Quant Spectrosc Radiat Transfer. — 1991. — Vol. 46. — P. 221–236.

Schaaf, C. B., Gao, F., Strahler, A. H., Lucht, W., Li, X., Tsang, T., Strugnell, N. C., Zhang, X., Jin, Y., Muller, J.-P., Lewis, P., Barnsley, M., Hobson, P., Disney, M., Roberts, G., Dunderdale, M., Doll, C., d'Entremont, R. P., Hu, B., Liang, S., Privette, J. L., and Roy, D.: First operational BRDF, albedo nadir reflectance products from MODIS, Remote Sensing of Environment, 83, 135 – 148, 2002.

Sinreich, R., U. Frieß, and U. Platt (2005), Multi axis differential optical absorption spectroscopy (MAX-DOAS) of gas and aerosol distributions, Faraday Discuss., 130, doi:10.1039/b419274p

Titov G.A. Statistical description of radiative transfer in clouds // J Atmos Sci. — 1990. — Vol. 47, no. 1. — P. 24–38

Trees, V. J. H., Wang, P., Stammes, P., Tilstra, L. G., Donovan, D. P., and Siebesma, A. P.: DARCLOS: a cloud shadow detection algorithm for TROPOMI, Atmos. Meas. Tech., 15, 3121–3140, https://doi.org/10.5194/amt-15-3121-2022, 2022.

van Geffen, J. H. G. M., Eskes, H. J., Boersma, K. F., and Veefkind, J. P.: TROPOMI ATBD of the total and tropospheric NO_2 data products, Report S5P-KNMI-L2-0005-RP, version 2.2.0, 2021-06-16, KNMI, De Bilt, The Netherlands, http://www.tropomi.eu/data-products/nitrogen-dioxide/ (last access: 7 March 2022), 2021.

van Geffen, J., Boersma, K. F., Eskes, H., Sneep, M., ter Linden, M., Zara, M., and Veefkind, J. P.: S5P TROPOMI NO_2 slant column retrieval: method, stability, uncertainties and comparisons with OMI, Atmos. Meas. Tech., 13, 1315–1335, https://doi.org/10.5194/amt-13-1315-2020, 2020.

van Geffen, J., Eskes, H., Compernolle, S., Pinardi, G., Verhoelst, T., Lambert, J.-C., Sneep, M., ter Linden, M., Ludewig, A., Boersma, K. F., and Veefkind, J. P.: Sentinel-5P TROPOMI NO_2 retrieval: impact of version v2.2 improvements and comparisons with OMI and ground-based data, Atmos. Meas. Tech., 15, 2037–2060, https://doi.org/10.5194/amt-15-2037-2022, 2022.

van Geffen, J.H.G.M., H.J. Eskes, K.F. Boersma, J.D. Maasakkers and J.P. Veefkind, TROPOMI ATBD of the total and tropospheric NO_2 data products, S5P-KNMI-L2-0005-RP, https://sentinel.esa.int/web/sentinel/technical-guides/sentinel-5p/products-algorithms, 2019.

Veefkind, J. P., de Haan, J. F., Sneep, M., and Levelt, P. F.: Improvements to the OMI O2–O2 operational cloud algorithm and comparisons with ground-based radar–lidar observations, Atmos. Meas. Tech., 9, 6035–6049, https://doi.org/10.5194/amt-9-6035-2016, 2016.

Verhoelst, T., Compernolle, S., Pinardi, G., Lambert, J.-C., Eskes, H. J., Eichmann, K.-U., Fjæraa, A. M., Granville, J., Niemeijer, S., Cede, A., Tiefengraber, M., Hendrick, F., Pazmiño, A., Bais, A., Bazureau, A., Boersma, K. F., Bognar, K., Dehn, A., Donner, S., Elokhov, A., Gebetsberger, M., Goutail, F., Grutter de la Mora, M., Gruzdev, A., Gratsea, M., Hansen, G. H., Irie, H., Jepsen, N., Kanaya, Y., Karagkiozidis, D., Kivi, R., Kreher, K., Levelt, P. F., Liu, C., Müller, M., Navarro Comas, M., Piters, A. J. M., Pommereau, J.-P., Portafaix, T., Prados-Roman, C., Puentedura, O., Querel, R., Remmers, J., Richter, A., Rimmer, J., Rivera Cárdenas, C., Saavedra de Miguel, L., Sinyakov, V. P., Stremme, W., Strong, K., Van Roozendael, M., Veefkind, J. P., Wagner, T., Wittrock, F., Yela González, M., and Zehner, C.: Ground-based validation of the Copernicus Sentinel-5P TROPOMI NO_2 measurements with the NDACC ZSL-DOAS, MAX-DOAS and Pandonia global networks, Atmos. Meas. Tech., 14, 481–510, https://doi.org/10.5194/amt-14-481-2021, 2021.

Vlemmix, T., Eskes, H. J., Piters, A. J. M., Schaap, M., Sauter, F. J., Kelder, H., and Levelt, P. F.: MAX-DOAS tropospheric nitrogen dioxide column measurements compared with the Lotos-Euros air quality model, Atmos. Chem. Phys., 15, 1313–1330, https://doi.org/10.5194/acp-15-1313-2015, 2015.

Vlemmix, T., Piters, A. J. M., Stammes, P., Wang, P., and Levelt, P. F.: Retrieval of tropospheric NO_2 using the MAX-DOAS method combined with relative intensity measurements for aerosol correction, Atmos. Meas. Tech., 3, 1287–1305, https://doi.org/10.5194/amt-3-1287-2010, 2010.

Wang, P., Stammes, P., van der A, R., Pinardi, G., and van Roozendael, M.: FRESCO+: an improved O2 A-band cloud retrieval algorithm for tropospheric trace gas retrievals, Atmos. Chem. Phys., 8, 6565–6576, https://doi.org/10.5194/acp-8-6565-2008, 2008.

Wang, Y., Beirle, S., Hendrick, F., Hilboll, A., Jin, J., Kyuberis, A. A., Lampel, J., Li, A., Luo, Y., Lodi, L., Ma, J., Navarro, M., Ortega, I., Peters, E., Polyansky, O. L., Remmers, J., Richter, A., Puentedura, O., Van Roozendael, M., Seyler, A., Tennyson, J., Volkamer, R., Xie, P., Zobov, N. F., and Wagner, T.: MAX-DOAS measurements of HONO slant column densities during the MAD-CAT campaign: inter-comparison, sensitivity studies on spectral analysis settings, and error budget, Atmos. Meas. Tech., 10, 3719–3742, https://doi.org/10.5194/amt-10-3719-2017, 2017.

Wissmeier, U.; Buras-Schnell, R.; Bernhard, M. PaNTICA: A fast 3D radiative transfer scheme to calculate surface solar irradiance for NWP and LES models. Journal of Applied Meteorology and Climatology 2013, 52, 1698-1715. 10.1175/JAMC-D-12-0227.1.

Wittrock, F., Oetjen, H., Richter, A., Fietkau, S., Medeke, T., Rozanov, A., and Burrows, J. P.: MAX-DOAS measurements of atmospheric trace gases in Ny-Ålesund - Radiative transfer studies and their application, Atmos. Chem. Phys., 4, 955–966, https://doi.org/10.5194/acp-4-955-2004, 2004.

Yang, P., Bi, L., Baum, B. A., Liou, K.-N., Kattawar, G., and Mishchenko, M.: Spectrally consistent scattering, absorption, and polarization properties of atmospheric ice crystals at wave-lengths from 0.2 µm to 100 µm, J. Atmos. Sci., pp. 330–347, 2013.

Zängle, G., Reinert, D., Ripodas, P., and Baldauf, M.: The ICON (ICOsahedral Non-hydrostatic) modelling framework of DWD and MPI-M: Description of the non-hydrostatic dynamical core, Quarterly Journal of the Royal Meteorological Society, 141, 563–579, https://doi.org/10.1002/qj.2378, 2015.

Yu, H., C. Emde, A. Kylling, B. Veihelmann, B. Mayer, K. Stebel, and M. Van Roozendael. Impact of 3D Cloud Structures on the Atmospheric Trace Gas Products from UV-VIS Sounders - Part II: impact on NO_2 retrieval and mitigation strategies. *Atmospheric Measurement Techniques Discussions*, 2021:1-34, 2021.